RESEARCH PAPER

Temperature-induced changes in the wheat phosphoproteome reveal temperature-regulated interconversion of phosphoforms

Lam Dai Vu[1,2,3,4,*], Tingting Zhu[1,2,3,4,*], Inge Verstraeten[1,2,†], Brigitte van de Cotte[1,2], The International Wheat Genome Sequencing Consortium[5], Kris Gevaert[3,4,‡] and Ive De Smet[1,2,‡,§]

[1] Ghent University, Department of Plant Biotechnology and Bioinformatics, B-9052 Ghent, Belgium
[2] VIB Center for Plant Systems Biology, B-9052 Ghent, Belgium
[3] Department of Biochemistry, Ghent University, B-9000 Ghent, Belgium
[4] VIB-UGent Center for Medical Biotechnology, B-9000 Ghent, Belgium
[5] Lee's Summit, MO 64086, USA

[†] Present address: Institute of Science and Technology Austria, 3400 Klosterneuburg, Austria.
* These authors contributed equally to this work.
[‡] These authors contributed equally to this work.
[§] Correspondence: ive.desmet@psb.vib-ugent.be

Abstract

Wheat (*Triticum* ssp.) is one of the most important human food sources. However, this crop is very sensitive to temperature changes. Specifically, processes during wheat leaf, flower, and seed development and photosynthesis, which all contribute to the yield of this crop, are affected by high temperature. While this has to some extent been investigated on physiological, developmental, and molecular levels, very little is known about early signalling events associated with an increase in temperature. Phosphorylation-mediated signalling mechanisms, which are quick and dynamic, are associated with plant growth and development, also under abiotic stress conditions. Therefore, we probed the impact of a short-term and mild increase in temperature on the wheat leaf and spikelet phosphoproteome. In total, 3822 (containing 5178 phosphosites) and 5581 phosphopeptides (containing 7023 phosphosites) were identified in leaf and spikelet samples, respectively. Following statistical analysis, the resulting data set provides the scientific community with a first large-scale plant phosphoproteome under the control of higher ambient temperature. This community resource on the high temperature-mediated wheat phosphoproteome will be valuable for future studies. Our analyses also revealed a core set of common proteins between leaf and spikelet, suggesting some level of conserved regulatory mechanisms. Furthermore, we observed temperature-regulated interconversion of phosphoforms, which probably impacts protein activity.

Keywords: Leaf, phosphoproteomics, phosphorylation, signalling, spikelet, temperature, wheat.

Introduction

Wheat (*Triticum* ssp.) is one of the most important staple food crops around the world (Hawkesford *et al.*, 2013). However, the current production of wheat is predicted to be insufficient to satisfy the future demands of the increasing world's population [Hawkesford *et al.*, 2013; Mochida and Shinozaki, 2013; International Wheat Genome Sequencing Consortium

(IWGSC), 2014]. In addition, global temperature is predicted to rise throughout the 21st century (IPCC, 2014), and it has been estimated that for each degree (°C) of temperature increase, global wheat production will reduce by 6%, thus impacting food security (Asseng *et al.*, 2015).

Wheat is sensitive to heat stress during all stages of its growth and development (Barber *et al.*, 2015; Akter and Rafiqul Islam, 2017). During wheat vegetative development, traits affected by high temperature include plant height, leaf weight, leaf width, relative water content, chlorophyll content, and secondary metabolites (Akter and Rafiqul Islam, 2017). Furthermore, generative wheat growth and development are also very susceptible to increased temperatures (Bennett *et al.*, 1971; Saini *et al.*, 1983, 1984; Draeger and Moore, 2017). Specifically, when wheat flowers are exposed to heat stress (10 °C above the optimum condition) between ear initiation and anthesis (i.e. when anther development goes through meiosis), this causes abnormal development of the pollen grains in the anther and subsequently results in grain yield reduction (Saini *et al.*, 1983; Saini *et al.*, 1984; Fischer, 1985; Wardlaw *et al.*, 1989). Heat can activate multiple signalling cascades, resulting in transcriptome, proteome, and metabolome changes (Rizhsky *et al.*, 2004; Yang *et al.*, 2011; Hasanuzzaman *et al.*, 2013; Asthir, 2015; de Leonardis *et al.*, 2015; Liu *et al.*, 2015; Zhang *et al.*, 2016, 2017). This leads to biosynthesis of HEAT SHOCK PROTEINs (HSPs), synthesis of antioxidants, and accumulation of osmoprotectants and solutes to reduce the negative effects of heat stress (Farooq *et al.*, 2011). For example, levels of various compounds that are beneficial for the plant during heat stress and known to protect the photosynthesis system increase in conditions of elevated temperature in *Arabidopsis thaliana*, wheat, and maize (Guy *et al.*, 2008; Scalabrin *et al.*, 2015; Qi *et al.*, 2017).

Lately, insight into the molecular and genetic control of plant thermomorphogenesis, a combination of morphological changes that contribute to adaptive growth acclimation to high ambient temperature conditions, has been growing (Quint *et al.*, 2016). This includes photoreceptors that function as thermosensors in *A. thaliana* (Jung *et al.*, 2016; Legris *et al.*, 2016; Hayes *et al.*, 2017), transcriptional regulators such as ELF3 and PIF4 in *A. thaliana* (Kumar *et al.*, 2012; Box *et al.*, 2015; Raschke *et al.*, 2015), the role of plant hormones (Gray *et al.*, 1998; Franklin *et al.*, 2011; Sun *et al.*, 2012; Wang *et al.*, 2016a; Ibañez *et al.*, 2018), and H2A.Z-containing nucleosomes that provide thermosensory information, which is used to co-ordinate the temperature transcriptome in *A. thaliana* and *Brachypodium* (Kumar and Wigge, 2010; Boden *et al.*, 2013). However, our knowledge of high temperature-associated signalling in crops, especially wheat, remains limited.

So far, transcriptome and proteome profiles have been investigated in wheat under heat stress, revealing differences in gene expression and protein levels, respectively (Liu *et al.*, 2015; Ahammed and Yu, 2016; Wang *et al.*, 2016b; Zhang *et al.*, 2016, 2017; Lu *et al.*, 2017). However, protein post-translational modifications (PTMs) are linked with plant stresses, and reversible protein phosphorylation in particular functions as a crucial regulatory mechanism in many biological processes (Hashiguchi and Komatsu, 2016), including the regulation of abiotic stress signalling in crops (Kline *et al.*, 2010; Bonhomme *et al.*, 2012;

Nguyen *et al.*, 2012; Yang *et al.*, 2013; Zhang *et al.*, 2014a, b; Ahammed and Yu, 2016; Zhen *et al.*, 2017). For example, phosphoproteome analyses of wheat under drought stress revealed a network of protein kinases and proteins involved in starch biosynthesis and grain development, the phosphorylation status of which is altered under these conditions (Zhang *et al.*, 2014b; Chen *et al.*, 2017). In the context of temperature, examples include phosphorylation of LATE EMBRYOGENESIS-abundant (LEA) proteins, which have been associated with wheat and barley tolerance to low temperatures (Kosová *et al.*, 2013), SNF1-RELATED PROTEIN KINASE 1 (SNRK1)-mediated phosphorylation of FUSCA3 (FUS3) under high temperature in *A. thaliana* (Chan *et al.*, 2017), and OPEN STOMATA 1 (OST1) and MITOGEN-ACTIVATED PROTEIN KINASE (MAPK)-mediated regulation of INDUCER OF CBP EXPRESSION 1 (ICE1) during cold signalling (Ding *et al.*, 2015; Li *et al.*, 2017; Zhao *et al.*, 2017). Taken together, PTMs—and specifically phosphorylation—have hardly been investigated in the context of high temperature stress (Wu *et al.*, 2016; Hashiguchi and Komatsu, 2016), especially in vegetative and reproductive organs of crop plants during development under high temperature (Kumar *et al.*, 2017). Nevertheless, understanding PTM-mediated signalling cascades associated with an elevated temperature response is essential to gain insight into thermal tolerance and to facilitate future breeding (Rampitsch and Bykova, 2012).

Here, we monitored phosphorylation events in leaves of wheat seedlings and wheat spikelets exposed for 1 h to higher temperature, and further analysed the data for biological processes potentially affected by phosphorylation. We identified a large number of phosphosites for proteins associated with diverse cellular and developmental functions, of which a subset showed a deregulated phosphostatus upon exposure to high temperature. Since research on PTMs of plant proteins, on temperature signalling and on wheat has been booming lately, we wanted to share this large resource of identified and temperature-regulated phosphorylation sites in wheat with the research community as soon as possible. Considering the number of phosphosites identified in our study, our results will be valuable for wheat (and by extension crop) research. This information already improved our understanding of the role of phosphorylation-mediated early signalling in wheat under high temperature stress. For example, we observed temperature-regulated interconversion of phosphoforms, especially of neighbouring phosphosites, which probably impacts protein activity.

Materials and methods

Wheat plant materials and growth conditions

The seeds used in this study were from two bread wheat (*Triticum aestivum*, AABBDD, $2n=6x=42$) cultivars, Fielder and Cadenza. The seeds were put on wet paper enclosed by plastic wrap and vernalized at 4 °C for 3–4 d, and then transferred to room temperature for germination. Seeds that germinated uniformly were selected and grown in plastic pots containing soil at 21 °C (Cadenza) or 24 °C (Fielder) under 16 h light/8 h dark (100 μE m^{-2} s^{-1} photosynthetically active radiation, supplied by cool-white fluorescent tungsten tubes, Osram), and 65–75% air humidity.

Temperature treatment

Temperature treatment was performed 8 h after the start of the light period. For the leaf material, Fielder plants at 7 d post-germination growing in separate pots were transferred to two incubators and grown at 34 °C (high temperature treatment) or 24 °C (control temperature) under constant light (100 µE m^{-2} s^{-1} photosynthetically active radiation) for 60 min. For the spikelet samples, Cadenza plants were cultivated in the greenhouse until the booting stage (stage 45 in Zadoks Decimal Code), then transferred to two incubators at 34 °C (high temperature treatment) and 21 °C (control temperature), respectively, under constant light (100 µE m^{-2} s^{-1} photosynthetically active radiation) for 60 min. The leaves of Fielder seedlings and the spikelets in the middle section of the ears from individual Cadenza plants were collected in three separate biological replicates and frozen in liquid nitrogen.

qRT-PCR

Three biological replicates were used per time point. RNA was extracted and purified with the RNeasy Mini Kit (Qiagen) according to the manufacturer's instruction for plant RNA extraction. DNA digestion was done on columns with RNase-free DNase I (Promega). The iScript cDNA Synthesis Kit (Biorad) was used for cDNA synthesis from 1 µg of RNA. qRT-PCR was performed on a LightCycler 480 (Roche Diagnostics) in 384-well plates with LightCycler 480 SYBR Green I Master reaction mix (Roche) according to the manufacturer's instructions. Two housekeeping genes, *ACTIN* (GenBank locus AB181991.1) and the *CELL DIVISION CONTROL PROTEIN* (*CDC*, GenBank locus EU267938.1) were used for normalization of the expression level of the *HSP* genes. All the primers are listed in Supplementary Table S1 available at *JXB* online.

Protein extraction and phosphopeptide enrichment

Total protein extraction was conducted on three biological replicate samples (leaf and spikelet material from independent plants) per wheat cultivar according to our previously described procedure with minor modifications (Vu *et al.*, 2017). Details can be found in the Supplementary Protocol S1. Phosphopeptides were enriched as previously described (Vu *et al.*, 2017).

LC-MS/MS analysis

Each sample was analysed via LC–MS/MS on an Ultimate 3000 RSLC nano LC (Thermo Fisher Scientific, Bremen, Germany) in-line connected to a Q Exactive mass spectrometer (Thermo Fisher Scientific). The peptides were first loaded on a trapping column [made in-house, 100 µm internal diameter (ID) ×20 mm, 5 µm beads C18 Reprosil-HD, Dr. Maisch, Ammerbuch-Entringen, Germany]. After flushing the trapping column, peptides were loaded in solvent A (0.1% formic acid in water) on a reverse-phase column (made in-house, 75 µm ID ×250 mm, 1.9 µm Reprosil–Pur–basic-C18-HD beads, Dr Maisch, packed in the needle) and eluted by an increase in solvent B (0.1% formic acid in acetonitrile) using a linear gradient from 2% solvent B to 55% solvent B in 120 min, followed by a washing step with 99% solvent B, all at a constant flow rate of 300 nl min^{-1}. The mass spectrometer was operated in data-dependent, positive ionization mode, automatically switching between MS and MS/MS acquisition for the five most abundant peaks in a given MS spectrum. The source voltage was set at 4.1 kV and the capillary temperature at 275 °C. One MS1 scan (m/z 400−2000, AGC target 3 × 10^6 ions, maximum ion injection time 80 ms), acquired at a resolution of 70 000 (at 200 m/z), was followed by five tandem MS scans (resolution 17 500 at 200 m/z) of the most intense ions fulfilling pre-defined selection criteria (AGC target 5 × 10^4 ions, maximum ion injection time 80 ms, isolation window 2 Da, fixed first mass 140 m/z, spectrum data type: centroid, under-fill ratio 2%, intensity threshold 1.3×E4, exclusion of unassigned, 1, 5–8, >8 positively charged precursors, peptide match preferred, exclude isotopes on, dynamic exclusion time 12 s). The HCD collision energy was set to 25% normalized collision energy and the

polydimethylcyclosiloxane background ion at 445.120025 Da was used for internal calibration (lock mass).

Database searching

MS/MS spectra were searched against the unpublished IWGSC RefSeq v1.0 database for *Triticum aestivum* (137 052 entries) (wheat-urgi.versailles. inra.fr/Seq-Repository/Assemblies) with the MaxQuant software (version 1.5.4.1), a program package allowing MS1-based label-free quantification acquired from Orbitrap instruments (Cox and Mann, 2008; Cox *et al.*, 2014). For comparison, a second search against the earlier version of the IWGSC PopSeq PGSB/MIPS v2.2 database (100 344 entries), downloaded from wheatproteome.org, was performed. Detailed MaxQuant settings can be found in Supplementary Protocol S1. All MS proteomics data have been deposited to the ProteomeXchange Consortium via the PRIDE partner repository (Vizcaíno *et al.*, 2014, 2016) with the data set identifier PXD008703. Next, the 'Phospho(STY).txt' output file generated by the MaxQuant search was loaded into the Perseus data analysis software (version 1.5.5.3) available in the MaxQuant package. Proteins that were quantified in at least two out of three replicates from each temperature were retained. Log2 protein ratios of the protein LFQ intensities were centred by subtracting the median of the entire set of protein ratios per sample. A two-sample test with a *P*-value cut-off of <0.01 was carried out to test for differences between the temperatures. Phosphopeptides with three valid values in one condition and none in the other were also retained and designated 'unique' for that condition.

In silico *analyses*

For Gene Ontology (GO) analysis, the protein sequences of all identified phosphoproteins were loaded in the BLAST2GO software and blasted against the NCBI non-redundant protein sequence database of green plants (*Viridiplantae*) with a cut-off E-value of 10^{-5}. Afterwards, the results were examined for GO annotation, and a Fisher's exact test (*P*<0.05) was performed to extract enriched GO terms in the regulated phospho-site data set. For Motif-X analyses, the Motif–X algorithm (Chou and Schwartz, 2011) was used to extract significantly enriched amino acid motifs surrounding the identified phosphosites. The sequence window was limited to 13 amino acids, and foreground peptides were pre-aligned with the phosphosite in the centre of the sequence window. All identified proteins were used as the background data set. The occurrence threshold was set at the minimum of 20 peptides and the *P*-value threshold was set at <10^{-6}. Structural modelling of the WD40 domain of *Ta*SPIRRIG was performed in SWISS-MODEL (Arnold *et al.*, 2006; Biasini *et al.*, 2014). The templates for the modelling studies were identified in the automated mode against the SWISS-MODEL template library (PDB: 5HYN). Structure representations were generated using the PyMOL Molecular Graphics System, Version 1.7.4, Schrödinger, LLC (www.pymol.org).

Results and Discussion

Experimental set-up for early leaf and spikelet phosphoproteome analyses

So far, our knowledge on changes in the wheat proteome upon elevated temperature is largely limited to long-term exposures (day or week long treatments; Majoul *et al.*, 2003; Laino *et al.*, 2010; Farooq *et al.*, 2011). We were interested in early signalling associated with a milder increase in ambient temperature, and therefore we wanted to profile changes in the phosphoproteome. To determine a suitable time point for proteome sampling, we first probed the expression levels of two *HSP* genes, since early thermal sensing is largely reflected in the transcription of *HSP* genes (Xu *et al.*, 2011). Here, we exposed 7-day-old wheat seedlings (Fielder) grown at 24 °C for a

short-term treatment of 34 °C and harvested whole shoots at different incubation times (Fig. 1A). Recent evidence in cereal crop plants has demonstrated a link between high temperature sensitivity at the booting stage and seed yield (Hedhly *et al.*, 2009; Draeger and Moore, 2017). Hence, we used booting wheat plants (Cadenza) grown at 21 °C and exposed to increased ambient temperature (34 °C), after which we harvested spikelets at different incubation times (Fig. 1B). Since developmental stages differ in optimal growth temperature (Porter and Gawith, 1999), we chose different optimal growth temperatures as the control conditions for our experiment. We analysed the transcription of *TaHSP70d* and *TaHSP90.1*, which are markers for temperature response (Xue *et al.*, 2014), in both leaf and spikelet samples. We found that the transcriptional response of *TaHSP70d* and *TaHSP90.1* peaked in both samples at 60 min, indicating a maximum of early high temperature response (Fig. 1C, D). Therefore, to identify early phosphorylation–controlled signalling components in wheat that are associated with a mild increased temperature, we subjected both leaf and spikelet samples from the 60 min time point to our phosphoproteomic workflow (Vu *et al.*, 2016).

New wheat reference sequence improves protein identification

Advances in the wheat reference sequence assembly provide a solid basis for proteome studies in wheat [Brenchley *et al.*, 2012; International Wheat Genome Sequencing Consortium (IWGSC), 2014; Luo *et al.*, 2017]. Through Ti–IMAC enrichment and subsequent LC–MS/MS analysis, we identified 3822 phosphopeptides containing 5178 phosphorylated amino acids, representing 2213 phosphoproteins in the leaf samples using the unpublished IWGSC RefSeq v1.0 assembly (Fig. 2; Supplementary Table S2). In spikelet samples, our workflow led to the identification of 5581 phosphopeptides containing 7023 phosphosites located on 2696 proteins (Fig. 2; Supplementary Table S3). As a comparison, we performed a second search using the earlier published protein sequence database based on the draft genome sequences of bread wheat [International Wheat Genome Sequencing Consortium (IWGSC), 2014]. The new protein database, based on the unpublished IWGSC RefSeq v1.0 assembly, resulted in an increase of 30% and 34% of identifications compared with the search using the previous search database that identified 3975 and 5234 phosphosites for leaf and spikelet samples, respectively. This seems to correlate with the increase of 36.5% in the number of entries in the new database compared with the old database, supporting the quality of the new wheat reference sequence assembly. To our knowledge, this is currently the largest set of identified phosphosites in the *Triticum* family. The identified phosphosites in this study were added to the PTMViewer (bioinformatics.psb.ugent.be/webtools/ptm_viewer/) (Vu *et al.*, 2016). In addition, we found several phosphosites that were differentially regulated between normal (21 °C or 24 °C) and increased ambient temperature (34 °C) in wheat leaves and spikelets (Fig. 2).

A temperature-regulated wheat leaf phosphoproteome

Phosphosites that exhibited valid values in one condition and none in the other indicate a massive change in phosphorylation levels. For the wheat leaves, we could identify 13 phosphosites that only occurred in the 34 °C condition and 32
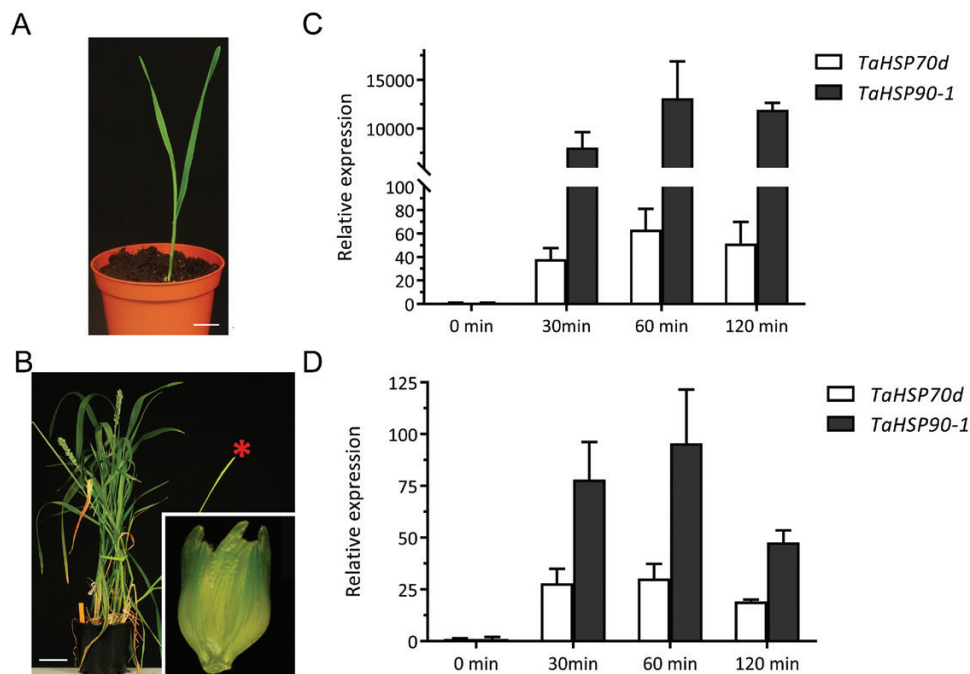
Fig. 1. Different wheat cultivars and organs used in this study. (A) Fielder seedlings are depicted at 7 d after germination. Scale bar=2.2 cm. (B) A Cadenza spikelet (inset) is depicted from plants at the booting stage. A red asterisk indicates a representative ear used for sampling. Scale bar=7.5 cm. (C and D) Analysis of *HSP70* and *HSP90* expression in both leaf and ear as a proxy for the heat sensing shows a maximum increase at 60 min after transferring to high temperature. (This figure is available in colour at *JXB* online.)
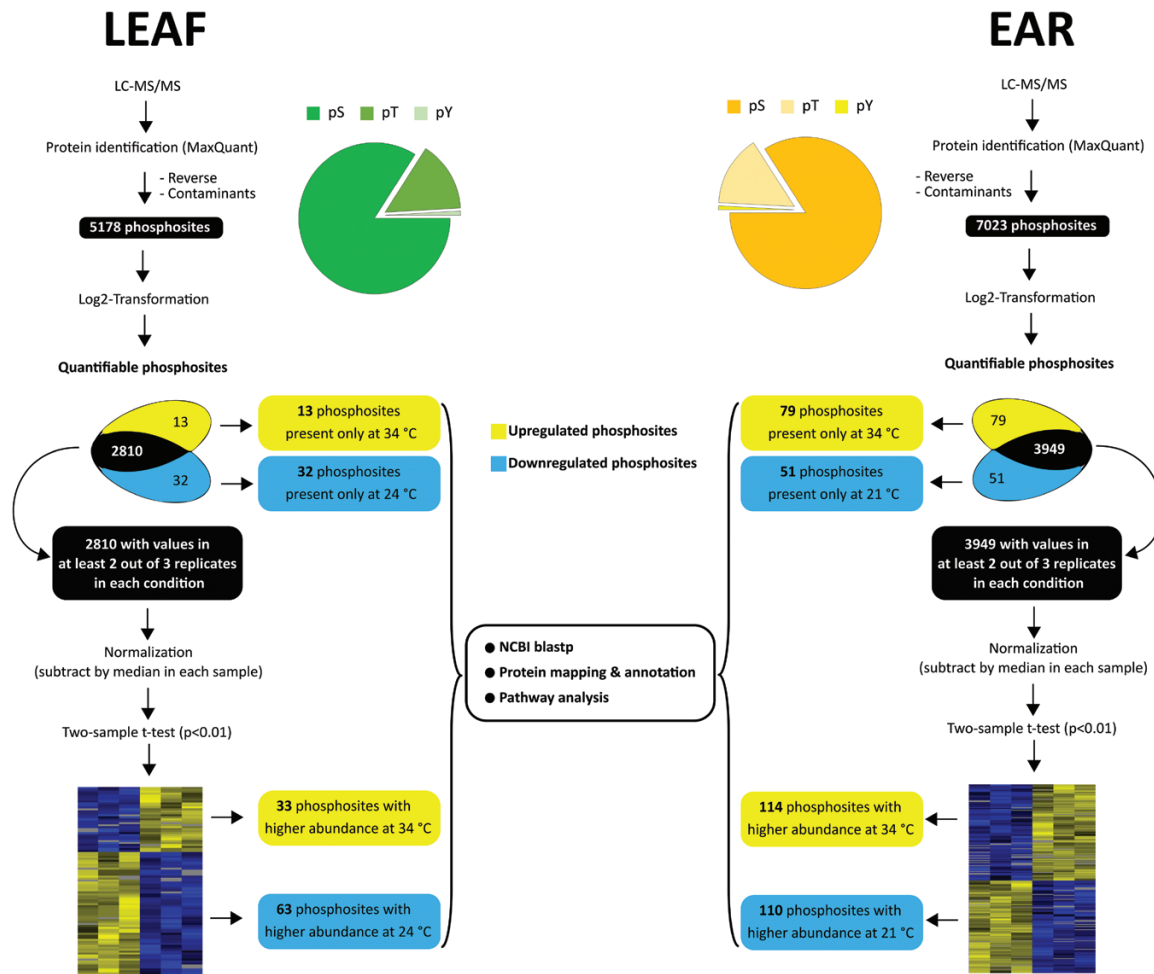
Fig. 2. Summary of the phosphoproteome analysis in wheat leaf and ear. *T*-test significant hits and phosphosites with valid values reproducibly present in only one condition in each organ are collectively analysed and called up-regulated or down-regulated phosphosites.

phosphosites that only occurred in the 24 °C condition (Fig. 2; Supplementary Table S4). On the rest of the wheat leaf data set, we performed a Student's *t*-test (*P*<0.01) on phosphosites with at least two valid values in any condition (2810 phosphosites), and this resulted in 33 significantly up-regulated phosphosites and 63 significantly down-regulated phosphosites upon high temperature (Supplementary Table S5). Proteins with phosphosites uniquely identified in either condition and significantly deregulated phosphoproteins from the statistical test were combined and analysed for over-represented GO terms in biological processes (Fig. 3) and molecular function (Supplementary Fig. S3). As expected, up-regulated phosphoproteins were highly enriched in the GO terms of stress-induced processes such as response to heat, protein folding (Zhu, 2016), response to hydrogen peroxide (Gupta *et al.*, 2016), and glucose transport (Ruan *et al.*, 2010). On the other hand, down-regulated phosphoproteins were mainly enriched in positive regulation of translational elongation/termination and ribosome biogenesis (Cherkasov *et al.*, 2015).

Expression of *HSP* genes was rapidly induced in the leaf by increased temperature (Fig. 1C), as the resulting proteins play crucial roles when plants are exposed to increased temperature (Sun *et al.*, 2002; Kotak *et al.*, 2007). In our leaf data

set, we identified several differential phosphorylation sites of HSPs at 34 °C (Supplementary Tables S4, S5); for example HSP90 (TraesCS2A01G033700.1, *Ta*HSP90) and HSP60-3A (TraesCSU01G009200.1, *Ta*HSP60-3A) were 10.4- and 4.6-fold up-regulated at S224 and S577, respectively. However, for both proteins, another phosphosite, namely S93 of *Ta*HSP90 and T420 of *Ta*HSP60-3A, was not differentially phosphorylated after 1 h exposure to 34 °C. This suggested that HSP90 and HSP60-3A protein abundance is probably not the basis for the increase in S224 and S577 phosphopeptide, respectively.

Noticeably, our data set indicated that the phosphoproteome of the photosynthesis machinery in wheat leaves is severely affected by high temperature, even under short-term exposure (Supplementary Tables S4, S5). For example, phosphorylation of T33, T37, and T39 of the subunit P of PHOTOSYSTEM I (TraesCS2A01G235000.1) was 3.2-fold down-regulated after 1 h exposure to 34 °C (Supplementary Table S5). In addition, an actin-binding protein (TraesCS1D01G422700.2), whose homologue in Arabidopsis [CHLOROPLAST UNUSUAL POSITIONING 1 (CHUP1)] is important for proper chloroplast positioning (Oikawa *et al.*, 2008), was found to be considerably less phosphorylated at S157 upon high temperature (Supplementary Table S4). In addition, a

A BIOLOGICAL PROCESS
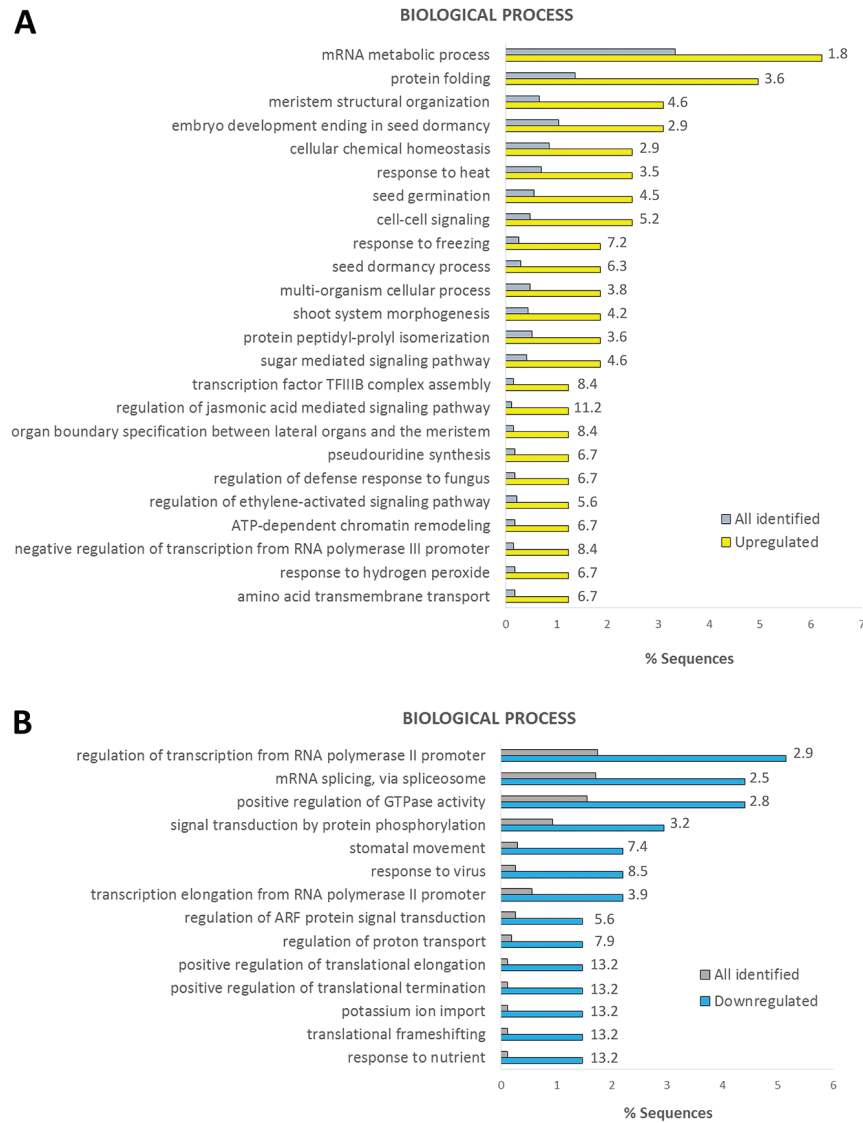

B BIOLOGICAL PROCESS
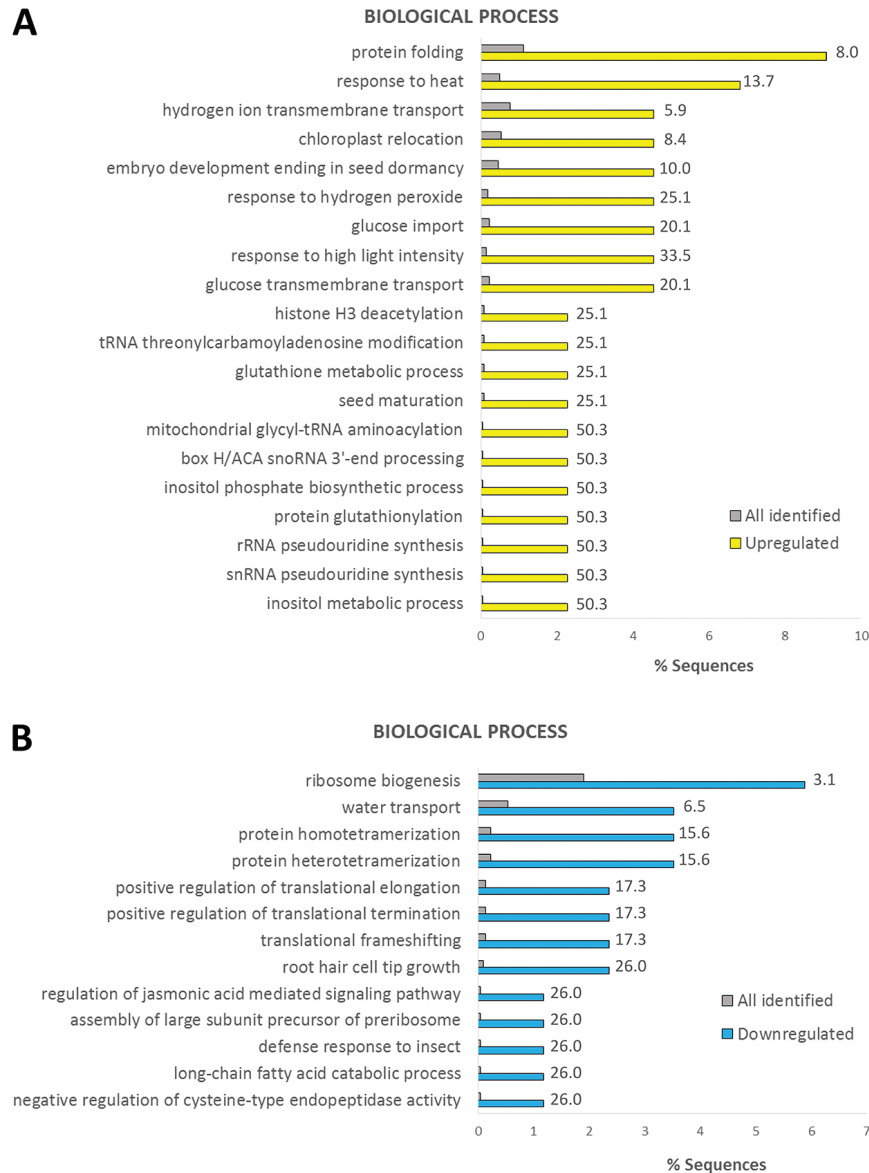
Fig. 3. GO enrichment for biological process in up-regulated (A) and down-regulated (B) phosphoproteins in leaf samples. All identified leaf phosphosites were used as the background data set. Fold change is indicated.

kinesin-like protein [TraesCS7D01G176200.1, homologous to Arabidopsis KINESIN LIKE PROTEIN FOR ACTIN BASED CHLOROPLAST MOVEMENT 1 (KAC1)] was highly phosphorylated in its kinesin motor domain (S444) in response to high temperature (Supplementary Table S4). Both CHUP1 and KAC1 regulate the accumulation of chloroplast actin filaments in Arabidopsis, thus facilitating the anchorage of chloroplasts on the plasma membrane. Lastly, phosphorylation of kinases involved in chloroplast movement, such as the phototropin homologues TraesCS5D01G389200.2 and TraesCS2B01G290500.3 (S525 and S294, respectively), was also elevated by heat (Supplementary Tables S4, S5).

The post-translational import of chloroplast proteins is a highly regulated process (Strittmatter *et al.*, 2010). Our data set showed several components of this process to be affected by high temperature. Increased temperature also highly induced the phosphorylation of a wheat homologue (TraesCS5D01G132600.1)

of Arabidopsis SERINE/THREONINE/TYROSINE KINASE 46 (STY46) at S31 (Supplementary Table S4). In Arabidopsis, STY46 and its homologues STY8 and STY17 facilitate the import of chloroplast pre-proteins by phosphorylation of their N-terminal transit peptide (Lamberti *et al.*, 2011). On the other hand, many chloroplast proteins are integrated into the chloroplast outer membrane (COM) without any cleavable signal sequence (Hofmann and Theg, 2005). The ANKYRIN REPEAT-CONTAINING PROTEIN 2 (AKR2) interacts with chloroplast-specific lipid markers and facilitates the insertion of proteins into the COM (Kim *et al.*, 2014). It is speculated that the regulatory mechanism of this process involves conformational changes of AKR2 via PTMs (Kim *et al.*, 2014). Here, we showed that phosphorylation of the AKR2 homologue in wheat (TraesCS4A01G328600.1) at S404 is 2-fold up-regulated in response to high temperature (Supplementary Table S5). While protein import in chloroplasts

Fig. 4. GO enrichment for biological process in up-regulated (A) and down-regulated (B) phosphoproteins in ear samples. All identified ear phosphosites were used as the background data set. Fold change is indicated.

has been shown to be altered under stress conditions (Dutta *et al.*, 2009; Ling and Jarvis, 2016), our data set indicated that this response, especially to high temperature, is highly regulated by phosphorylation.

In conclusion, our temperature-mediated leaf phosphoproteome pinpointed photosynthesis as a central target of higher temperature and identified several phosphorylated residues on key components for further functional characterization.

A temperature-regulated wheat spikelet phosphoproteome

For the wheat spikelet, we identified 79 phosphosites that were only present in the 34 °C samples and 51 phosphosites that were only present in the 21 °C samples (Fig. 2; and Supplementary Table S6). A Student's *t*-test (*P*<0.01) was performed on the rest of the wheat spikelet data set (phosphosites with at least two valid values in one temperature condition; 3949 phosphosites), and this resulted in 114 and 110 significantly up- and down-regulated phosphosites at elevated temperature, respectively (Supplementary Table S7). Proteins with phosphosites uniquely identified in either condition and significantly deregulated phosphoproteins from the statistical test were combined, and GO analysis was performed in a similar way as for the leaf samples (Fig. 4; Supplementary Figure S4). The biological processes enriched in leaf samples were also increased here, such as protein folding, response to heat, and response to hydrogen peroxide. Similar to the leaf GO enrichment (Fig. 3), terms associated with translation were predominantly enriched for down-regulated phosphoproteins.

Several phosphopeptides assigned to the auxin transporter PIN-FORMED1 (PIN1) homologue TraesCS6A01G308600.1 were identified in our data set (Supplementary Table S3). PIN-mediated auxin transport is controlled by phosphorylation, and several PIN1 phosphosites and associated regulatory kinases have been identified (Huang *et al.*, 2010; Facette *et al.*, 2013; Zourelidou *et al.*, 2014; Ahammed and Yu, 2016; Jia *et al.*, 2016; Ki *et al.*, 2016; Weller *et al.*, 2017; Dory *et al.*, 2018). Upon high

temperature, phosphorylation of S268/S269 and T284 showed increased abundance (Supplementary Table S7). These residues are conserved among different plant species (Supplementary Fig. S5). In Arabidopsis, the corresponding phosphosite for S269 belongs to a phosphorylation motif of the D6 protein kinases (D6PKs) (Zourelidou *et al.*, 2014), and the corresponding phosphosite for T284 has been shown to be one of the direct targets of the mitogen-activated protein kinases MPK4 and MPK6 (Jia *et al.*, 2016; Dory *et al.*, 2018). Interfering with the corresponding *At*PIN1 phosphosites of S269 shows an impaired auxin efflux activation by D6PKs (Zourelidou *et al.*, 2014), and phosphomimetic mutants of the MPK4/6-regulated PIN1 phosphosites show an intracellular relocalization of PIN1 from the plasma membrane (Dory *et al.*, 2018). Since MAPK cascades are activated by various abiotic stresses (de Zelicourt *et al.*, 2016), this might provide a link between stress-induced regulation of auxin transport that affects plant development, in this case a high temperature stress-induced alteration of inflorescence development that largely depends on PIN1 activity (Galli *et al.*, 2015; O'Connor *et al.*, 2017). Further, reproductive development in plants is known to be greatly dependent on the epigenetic control of expression of flowering genes (Gan *et al.*, 2013). This often involves histone modifications such as (de)acetylation, methylation, and ubiquitination (Lawrence *et al.*, 2016). Here, we found that the phosphorylation of several histone-modifying enzymes was deregulated in response to heat. For example, the phosphoserine 297 of the histone deacetylase TraesCS1A01G445700.3 was 7.1-fold down-regulated and the phosphorylation of S762/S763 in the histone–lysine *N*-methyltransferase TraesCS2A01G262600.1 was 2.4-fold decreased (Supplementary Table S7). In contrast, a ubiquitin protease, TraesCS4D01G266600.3, was 2.2-fold more phosphorylated at S31 and T32. Its Arabidopsis homologue, UBIQUITIN-SPECIFIC PROTEASE 26 (UBP26), deubiquitinates the histone H2B to regulate floral transition by controlling the expression of *FLOWERING LOCUS C* (*FLC*) (Schmitz *et al.*, 2009). Furthermore, it has been demonstrated that phosphorylation is crucial for the activity of histone-modifying enzymes (Pflum *et al.*, 2001; Schmitz *et al.*, 2009; Xu *et al.*, 2015).

Another important step in epigenetic control of gene expression is the ATP-dependent restructuring of nucleosomes (Vignali *et al.*, 2000). Phosphorylation of two homologous SWI2/SNF2 class of chromatin remodelling ATPases, TraesCS7D01G206700.3 (at T2492) and TraesCS7B01G110600.1 (at S1668 and S1671), was massively induced by heat (Supplementary Table S6). The Arabidopsis homologue, SPLAYED (SYD), is known to be a co-repressor during floral transition (Wagner and Meyerowitz, 2002). In contrast, phosphorylation of S1728 in the SNF2 ATPase TraesCS6B01G048200.2 was 1.7-fold down-regulated (Supplementary Table S7). Its homologue in Arabidopsis, BRAHMA (BRM), plays a pivotal role in controlling flowering time by regulating the expression of *FLC* and inflorescence architecture, mainly via interaction with the transcription factor KNOTTED-LIKE FROM ARABIDOPSIS THALIANA 1 (KNAT1) (Zhao *et al.*, 2015). Interestingly, a wheat homologue

of KNAT1, TraesCS5B01G410600.1, was also less phosphorylated at high temperature (Supplementary Table S7).

In conclusion, our data suggested that an increase in ambient temperature can alter the phosphorylation status of chromatin remodelling proteins as an important mechanism to control gene expression during the reproductive stage. Further, other proteins involved in pollen, pistil, or gametophyte development (Supplementary Tables S6, S7) also exhibited altered phosphorylation in response to increased temperature.

Comparison of the leaf and spikelet phosphoproteome

In total, we identified 2491 identical phosphosites in both organs, which account for 48% and 35% of all identified phosphosites in leaf and spikelet samples, respectively (Fig. 5). Only seven phosphosites were found commonly up-regulated at high temperature in both organs, and eight were commonly down-regulated in both organs (Fig. 5; Supplementary Table S8). Notwithstanding the considerable overlap between the phosphosites identified in both organs, the limited overlap between similarly regulated phosphosites indicated distinct responses in the leaf and spikelet phosphoproteomes at the early stages of thermal signalling.

Among the common high temperature-induced phosphosites, phosphorylation of S464 of the pseudouridine synthase TraesCS2B01G177000.1 was increased 1.6-fold and 1.9-fold
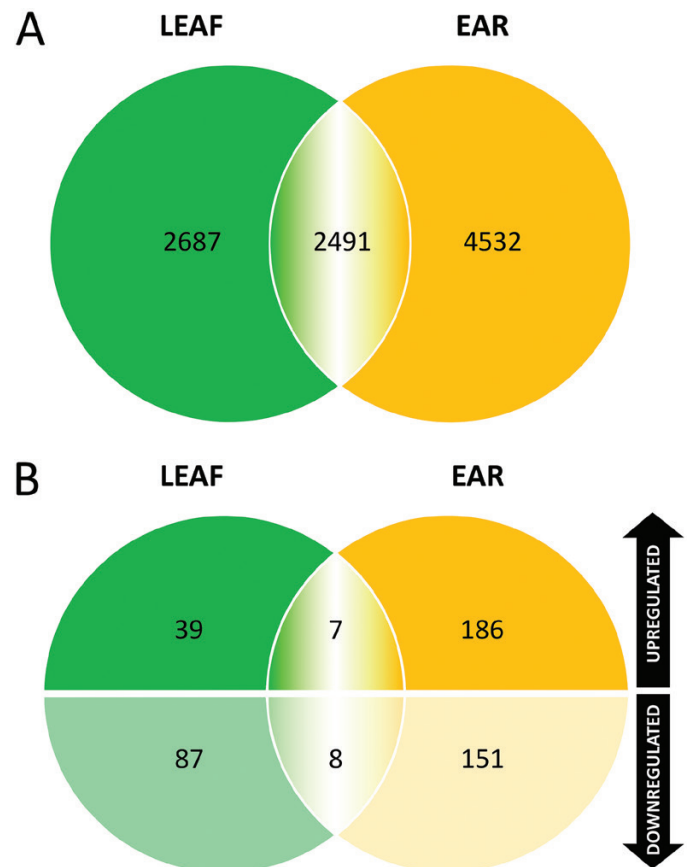
Fig. 5. Venn diagrams showing the number of common identified phosphosites as well as deregulated phosphosites in leaf and ear samples.

in leaf and spikelet samples, respectively. Pseudouridylation of mRNA as well as of non-coding RNAs can be induced in stress conditions and is important for the regulation of gene expression, and involved in splicing, translation, and decay of mRNA (Karijolich *et al.*, 2015). On the other hand, three different translation initiation factors were present among the commonly regulated proteins with down-regulated phosphosites (Supplementary Table S8). This is in agreement with heat stress-triggered overall pausing of translation elongation, and with heat-induced HSP70 protecting cells from heat shock-induced pausing (Shalgi *et al.*, 2014; Merret *et al.*, 2015). In particular, dephosphorylation of translation initiation factors correlates with the reprogramming of translation following thermal stress in wheat (Gallie *et al.*, 1997).

Leaf and spikelet phosphoproteome Motif-X analyses reveal distinct regulation of phosphorylation motifs

So far, little is known about the protein kinases and phosphatases involved in temperature signalling (Ding *et al.*, 2015; Li *et al.*, 2017; Yu *et al.*, 2017; Zhao *et al.*, 2017). Therefore, we used the identified phosphosites to reveal potential phosphorylation motifs and associated kinases that may act in a high-temperature-responsive manner. The Motif-X algorithm was applied on the set of regulated phosphosites in leaf and spikelet samples separately, using the sequences of all identified phosphoproteins in either organ as a reference (Fig. 6). In the spikelet, the common SP motif was enriched in both up-regulated and down-regulated phosphosites. This suggested that kinases (and phosphatases) targeting those sites are tightly regulating the protein phosphorylation signatures (meaning the specific combination of phosphorylated and non-phosphorylated residues), which impacts on overall protein behaviour, such as protein activity and localization (Salazar and Höfer, 2009). The acidic SD motif was significantly over-represented among the up-regulated phosphosites (3.61-fold). In contrast,

the down-regulated phosphosites showed enrichment in the basic RxxS motif (4.37-fold) (Fig. 6). This latter trend was also found in the leaf samples (Fig. 6). Despite the fact that no motif enrichment was obtained for the up-regulated phosphosites in leaf samples, due to the small size of the data set, we identified six SD motifs among these sites, which account for 13% of the up-regulated phosphosites in leaves. This was comparable with 14% of the up-regulated phosphosites in the spikelet samples which also show the SD motif. This possibly indicated a common molecular mechanism of high temperature response via phosphorylation across different organs and different growth stages. While local intracellular parameters such as the pH can slightly vary in a temperature-dependent manner and thus affect the property of amino acid residues around the phosphosites (Wilkinson, 1999; Schönichen *et al.*, 2013), we do not rule out the possibility that certain phosphosites are targeted by a specific set of high temperature-activated kinases. The acidic motif SD is known to be targeted by MAP kinases (MPKs), receptor-like kinases (RLKs), and calcium-dependent protein kinases (CDPKs), while RxxS is a motif commonly targeted by MAP kinase kinases (MAP2Ks) (van Wijk *et al.*, 2014). In support of this, we found six RLKs among 10 kinases with a higher phosphorylation level at 34 °C in the spikelets, whereas three out of seven kinases with a decreased phosphorylation level are predicted to have MAP3K or MAP4K activity (Supplementary Table S9).

Phosphoproteins with multiple deregulated phosphosites

Since the protein phosphosignature will determine protein behaviour (Salazar and Höfer, 2009), we probed the leaf and spikelet phosphoproteome data for proteins that displayed a combination of up- and down-regulated phosphosites. We found 13 phosphoproteins in the spikelet samples and one in the leaf samples that contained both significantly up- and
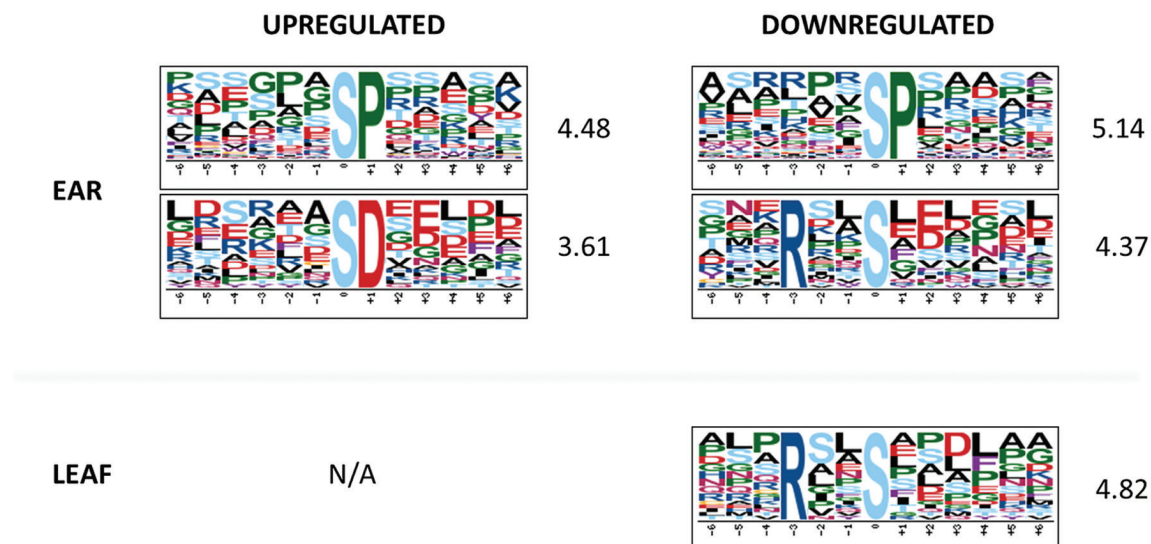
Fig. 6. Motif-X analysis show an enrichment of an acidic phosphomotif among up-regulated phosphosites and of a basic motif among down-regulated phosphosites in leaf and ear. Fold change of the enrichment compared with the background data set is indicated. N/A, not available.

down-regulated phosphosites (Table 1). It is thus very likely that the status of these phosphosites is not affected by changes in the protein level, but rather by high temperature-dependent activity of associated kinases and phosphatases. These protein phosphatases and kinases might be activated by high temperature and target the phosphosites independently to generate different phosphoforms of the target protein (Fig. 7A). However, the phosphorylation and dephosphorylation events might also occur in an interdependent manner upon high temperature (Fig. 7B) (Salazar and Höfer, 2009; Nishi *et al.*, 2015). Crosstalk between different types or the same type of PTMs is very common (Beltrao *et al.*, 2013; Nishi *et al.*, 2015), but is still not widely explored in plants.

A complex example is the putative protein kinase TraesCS6B01G377500.3 (Table 1), which exhibited two phosphosites S711 and S762 that were respectively, 2.6- and 2.1-fold up-regulated in the spikelet samples treated at 34 °C.

In contrast, a doubly phosphorylated peptide (DFPI*pS*PS*pS*AR, S227 and S230) was detected at a 2.5-fold higher level in the 21 °C samples. Further, a single peptide (*pS*SGIETTPAEAE-ALSK or S*pS*GIETTPAEAEALSK) could only be detected for all 21 °C samples, albeit the phosphosite could not be exactly localized (either S768 or S769).

In addition, we also found proteins with multiple phosphosites that showed the same deregulation across different temperatures (Supplementary Table S10). A large portion of these sites were detected together on the multi-phosphorylated peptides. These phosphosites may work synergistically to control the protein function at elevated temperature or may generate a phosphorylation code for crosstalk between different protein kinases or phosphatases as discussed above. However, in this case, a change in protein level may result in a general change in abundance of the phosphopeptide pool. Hence, studying the co-regulation of these phosphosites will require additional

Table 1. List of phosphoproteins exhibiting multiple up-regulated and down-regulated phosphosites

Wheat ID	Up-regulated	Fold change (up-regulation)	Down-regulated	Fold change (down-regulation)	Arabidopsis homologues	Arabidopsis homologue description
TraesCS2A01G209100.1	T1371	5.5	S969	2.7	AT3G60240	CUM2, protein synthesis initiation factor 4G
TraesCS2D01G281200.1	S12[a]	Unique for 34 °C	S12[a] S10	3.4 3.4	AT5G51300	ATSF1, nuclear localized splicing factor, involved in alternative splicing of some mRNAs.
TraesCS3A01G538200.1	S1297	Unique for 34 °C	S1126	2.4	AT3G09670	Tudor/PWWP/MBT superfamily protein
TraesCS3B01G212100.3	S771	Unique for 34 °C	T606	Unique for 21 °C	AT5G21160	LARP1a, involved in mRNA degradation in response to heat stress.
TraesCS3D01G178100.1	S5 S6	Unique for 34 °C Unique for 34 °C	S203	5.1	AT3G62330	OXS2, zinc finger family protein
TraesCS3D01G205900.4	S648	Unique for 34 °C	S672	1.6	AT3G06670	SMEK1, forms complex with PP4 proteins to target and dephosphorylate HYL1 which in turn promotes miRNA biogenesis.
TraesCS3D01G230600.1	T4	Unique for 34 °C	S210	Unique for 21 °C	AT1G60690	NAD(P)-linked oxidoreductase
TraesCS4D01G034300.1	S152	1.5	S575	3.5	AT2G41900	CCCH-type zinc finger protein
TraesCS5B01G387800.1	S3236	Unique for 34 °C	T3238	Unique for 21 °C	AT1G03060	SPIRRIG, WD/BEACH domain protein
TraesCS6B01G208900.5	S363 T360	2.0 2.0	S439	1.5	AT3G63400	Cyclophilin-like peptidyl-prolyl *cis-trans* isomerase
TraesCS6B01G377500.3	S711 S762	2.6 2.1	S768 /S769 S227 S230	Unique for 21 °C 2.5 2.5	AT5G57610	Kinase superfamily protein
TraesCS6D01G167200.1	S791 S794 S348 T345	13.9 13.9 2.0 2.0	S424	1.5	AT3G63400	Cyclophilin-like peptidyl-prolyl *cis-trans* isomerase
TraesCS7B01G002900.1	S460	Unique for 34 °C	S249	3.41	AT5G43310	COP1-interacting protein-like protein
TraesCS5A01G291600.1	S572	Unique for 34 °C	S485 S486	1.38 1.38	AT2G33490	Hydroxyproline-rich glycoprotein family protein

[a] For TraesCS2D01G281200.1, the peptide containing only phosphorylated S12 is up-regulated and the doubly phosphorylated peptide (S12 and S10) is down-regulated.
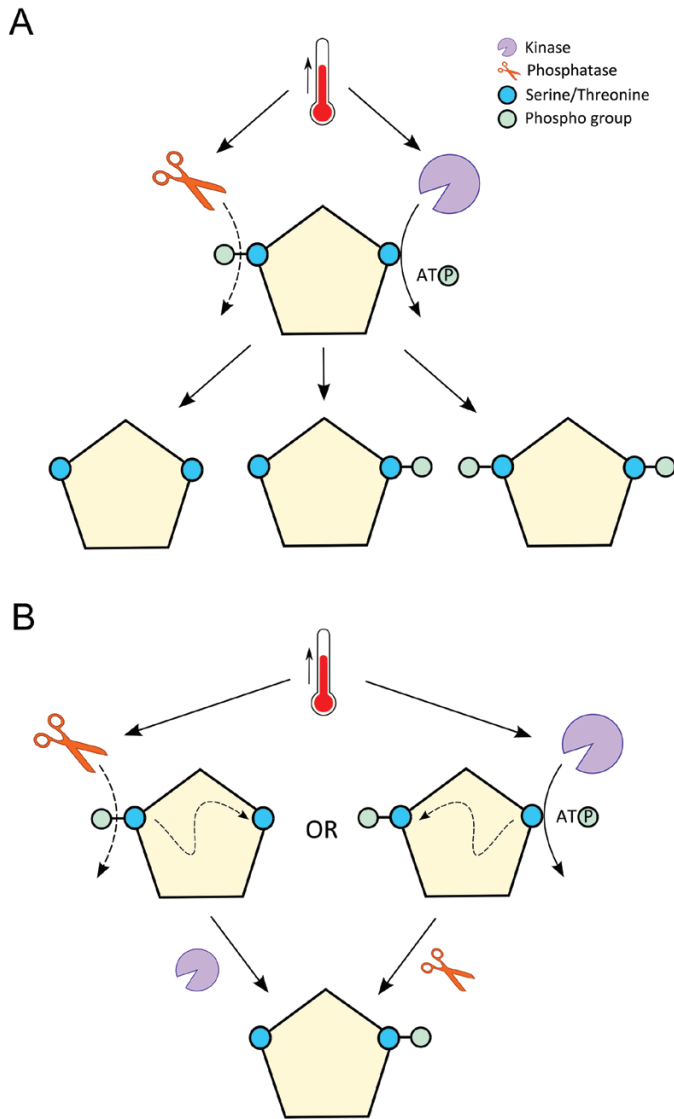
Fig. 7. Heat-dependent phosphorylation and dephosphorylation on a single target protein. (A) Heat activates both the kinase and the phosphatase to target different serine or threonine residues simultaneously, generating different phosphoforms of the protein. (B) First, heat activates the phosphatase or kinase. The dephosphorylation or phosphorylation of the protein serves as a crosstalk signal for a second kinase or phosphatase to operate, generating one single phosphoform of the protein.

investigation on the abundance of the associated proteins, for example by analysing intact proteins or rather the different proteoforms.

Altogether, our data indicated that multiple phosphorylation/dephosphorylation events of a single protein induced by stress are common and add another level of complexity to our understanding of stress signalling mechanisms in plants.

Temperature-induced interconversion of neighbouring phosphorylation residues

Interestingly, in the spikelet samples, TraesCS5B01G387800.1 (Table 1), which is a homologue of the WD40/BEACH domain

protein SPIRRIG in *A. thaliana*, exhibited two phosphosites in close proximity with opposite differential regulation upon high temperature. The phosphosite S3236 (*pS*PTTTYGG-PGLDVQTLEYR) could only be detected at 34 °C, whereas the phosphosite T3238 (SP*pT*TTYGGPGLDVQTLEYR) could only be detected at 21 °C (Supplementary Fig. S6). The phosphosites are located in the WD40-repeat domain (Fig. 8A), which is crucial for interaction of SPIRRIG with the decapping protein DECAPPING 1 (DCP1) to regulate mRNA decay upon salt stress in Arabidopsis (Steffens *et al.*, 2015).

Inspecting the protein sequence, we found the two phosphorylation sites localized in a sequence window of 10 amino acids of which four are either serine or threonine (Fig. 8B). Neither phosphorylation of the two other threonine residues nor a hyper-phosphorylated species of the same peptide could be detected. Hence, a combined effect of phosphorylation of individual sites is probably not relevant. The S3236 residue was and the T3238 residue was not conserved among SPIRRIG homologues, but we found a high frequency of serine and threonine residues in the same sequence windows in other seed plants (Fig. 8B). While the high occurrence of phosphorylatable residues might help to preserve the functional phosphorylation pool of a particular sequence during evolution, we suspect that the conformational change of the protein upon stimuli such as heat could lead to the preference for one phosphosite over the other by the same kinase. This might provide a buffering mechanism to maintain the function of the protein by differential phosphorylation of neighbouring amino acid residues depending on the environmental conditions. However, we also do not rule out allosteric or orthosteric regulation between the two phosphosites that might affect the activity of the protein (Nussinov *et al.*, 2012).

For the splicing factor TraesCS2D01G281200.1 (Table 1), the peptide containing only phosphorylated S12 (ASAETLARSP*pS*REPSSDPPR) was uniquely detected at 34 °C, while the doubly phosphorylated peptide of S10 and S12 (ASAETLAR*pS*P*pS*REPSSDPPR) was 3.4-fold down-regulated at the same temperature in the spikelets. We speculate that the phosphoforms of TraesCS2D01G281200.1 may co-exist in a temperature-dependent stoichiometry.

Such interconversion of neighbouring phosphorylation residues (Fig. 8C) has until now seldom been observed. One example can be found in the cyanobacterium *Synechococcus elongatus*, where the circadian clock is controlled by the oscillating phosphorylation equilibrium between a neighbouring serine and threonine in the protein kinase KaiC (Rust *et al.*, 2007). This phosphorylation switch between the two residues is modulated by the stoichiometric interaction of KaiC with KaiA and KaiB, in which the pS-KaiC form antagonizes KaiA activity, whereas the pT-KaiC form does not. Similarly, a dual phosphorylation switch has been studied in human (Kilisch *et al.*, 2016). To our knowledge, similar phosphorylation modules have not been reported in plants, especially not in the context of stress responses. It is possible that temperature serves as a signalling switch for such a phosphorylation toggle via regulated interaction with at least a protein kinase and/or phosphatase.
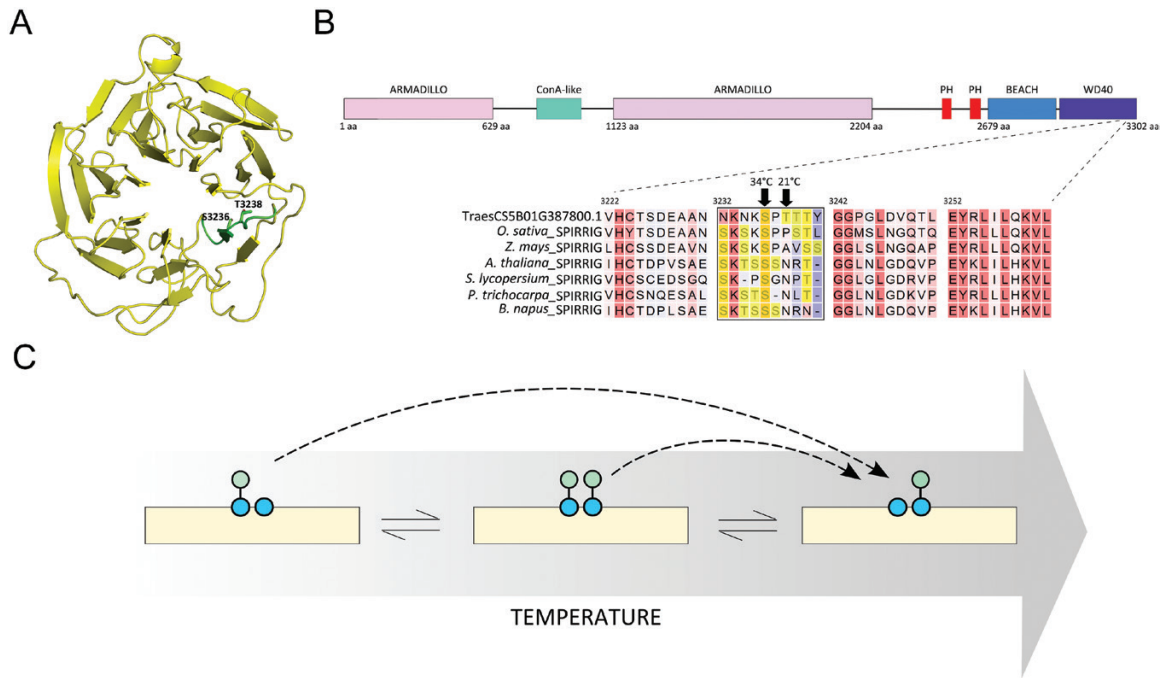
Fig. 8. (A) Structural model of the WD40 domain of *Triticum aestivum* SPIRRIG (TraesCS5B01G387800.1). The Ser/Thr-rich sequence is highlighted in green, showing the two phosphosites detected in the study. (B) Alignment of SPIRRIG homologues from different plant species. The Ser/Thr-rich window is marked, with the Ser/Thr residues highlighted in yellow. Domain prediction was performed in Interpro (http://www.ebi.ac.uk/interpro/). (C) Model of temperature-induced interconversion of neighbouring phosphosites.

Conclusion

In conclusion, we provide the scientific community with the first large-scale phosphoproteome in plants under the control of high ambient temperature across different temperature-sensitive organs. An in-depth analysis showed that the photosynthetic machinery in the leaf is highly responsive to increased temperature, while epigenetic regulation in the spikelets seems to be tightly regulated by high temperature in a phosphorylation-dependent manner during reproductive development. In future, it will be exciting to explore the functional role of specific phosphorylation events in controlling conserved physiological processes, such as PIN-mediated auxin transport, but also PLASMA MEMBRANE INTRINSIC PROTEIN (PIP)-mediated water transport or PSII activity, upon exposure of wheat plants to high temperature. Furthermore, we observed a core set of common proteins between both leaf and spikelet, suggesting some conserved mechanisms in these organs when responding to high temperature. Nevertheless, we also observed a large portion of organ-specific regulation. Given that temperature has a major impact on plant fertility at various levels, including pollen abortion, formation of sterile pollen, malformation of the spindle during meiosis impacting viability and ploidy of gametes, and degeneration of tapetum tissue (Saini *et al.*, 1984; Suzuki *et al.*, 2001; Jagadish *et al.*, 2007; Zinn *et al.*, 2010; Pécrix *et al.*, 2011; De Storme and Geelen, 2014; Wang *et al.*, 2017), our data set identifies phosphorylated proteins likely to be involved in these processes. Finally, we exposed a, so far, not reported mechanism of interconversion of neighbouring phosphorylation residues, which probably plays a key role in temperature signalling. Taken together, our data set increases the understanding of temperature signalling in plants and provides the wheat community with putative phosphoprotein-based biomarkers that can facilitate breeding to improve temperature-related agronomic wheat properties.

Supplementary data

Supplementary data are available at *JXB* online.

Table S1. Primers used in this study.

Table S2. Phosphosites identified in wheat leaves.

Table S3. Phosphosites identified in wheat spikelets.

Table S4. Phosphosites uniquely present at either 24 °C or 34 °C in wheat leaves.

Table S5. Phosphosites significantly deregulated at 34 °C (Students' *t*-test $P<0.01$) in wheat leaves.

Table S6. Phosphosites uniquely present at either 21 °C or 34 °C in wheat spikelets.

Table S7. Phosphosites significantly deregulated at 34 °C (Students' *t*-test $P<0.01$) in wheat spikelets.

Table S8. Phosphosites commonly up-regulated or down-regulated at 34 °C in both leaves and spikelets

Table S9. Kinases with deregulated phosphosites in this study.

Table S10. List of proteins with multiple up-regulated or multiple down-regulated phosphosites.

Fig. S1. Summary of the phosphoproteomic workflow.

Fig. S2. Histograms show normal distribution of log2 intensity of quantifiable proteins (proteins present in only one of two temperatures or having at least two valid values per temperature) in leaf (A) and spikelet (B)

Fig. S3. Over-represented GO terms for molecular functions among leaf proteins with (A) up-regulated or (B) down-regulated phosphosites. Fold changes are indicated.

Fig. S4. Over-represented GO terms for molecular functions among spikelet proteins with (A) up-regulated or (B) down-regulated phosphosites. Fold changes are indicated.

Fig. S5. Conserved high temperature-regulated *Triticum aestivum* PIN1 phosphosites.

Fig. S6. Mass spectrum of phosphopeptides containing S3236 (A) and T3238 (B) in SPIRRIG homologue TraesCS5B01G387800.1.

Protocol S1.

Dataset S1.

Acknowledgements

Authors contributions

LDV and TZ performed the experiments, analysed data, wrote the manuscript, and contributed equally. IV performed experiments and critically revised the manuscript. BVDC performed the experiments. IWGSC generated and provided access to the new wheat genome annotation. IDS and KG designed and co-ordinated the research, wrote the manuscript, and contributed equally.

References

Ahammed GJ, Yu JQ, **eds.** 2016. Plant hormones under challenging environmental factors. Dordrecht: Springer Netherlands.

Akter N, Rafiqul Islam M. 2017. Heat stress effects and management in wheat. A review. Agronomy for Sustainable Development **37,** 1–17.

Arnold K, Bordoli L, Kopp J, Schwede T. 2006. The SWISS-MODEL workspace: a web-based environment for protein structure homology modelling. Bioinformatics **22,** 195–201.

Asseng S, Ewert F, Martre P, et al. 2015. Rising temperatures reduce global wheat production. Nature Climate Change **5,** 143–147.

Asthir B. 2015. Protective mechanisms of heat tolerance in crop plants. Journal of Plant Interactions **10,** 202–210.

Barber HM, Carney J, Alghabari F, Gooding MJ. 2015. Decimal growth stages for precision wheat production in changing environments? Annals of Applied Biology **166,** 355–371.

Beltrao P, Bork P, Krogan NJ, van Noort V. 2013. Evolution and functional cross-talk of protein post-translational modifications. Molecular Systems Biology **9,** 714.

Bennett MD, Chapman V, Riley R. 1971. The duration of meiosis in pollen mother cells of wheat, rye and Triticale. Proceedings of the Royal Society B: Biological Sciences **178,** 259–275.

Biasini M, Bienert S, Waterhouse A, et al. 2014. SWISS-MODEL: modelling protein tertiary and quaternary structure using evolutionary information. Nucleic Acids Research **42,** W252–W258.

Boden SA, Kavanová M, Finnegan EJ, Wigge PA. 2013. Thermal stress effects on grain yield in *Brachypodium distachyon* occur via H2A.Z-nucleosomes. Genome Biology **14,** R65.

Bonhomme L, Valot B, Tardieu F, Zivy M. 2012. Phosphoproteome dynamics upon changes in plant water status reveal early events associated with rapid growth adjustment in maize leaves. Molecular and Cellular Proteomics **11,** 957–972.

Box MS, Huang BE, Domijan M, et al. 2015. ELF3 controls thermoresponsive growth in Arabidopsis. Current Biology **25,** 194–199.

Brenchley R, Spannagl M, Pfeifer M, et al. 2012. Analysis of the bread wheat genome using whole-genome shotgun sequencing. Nature **491,** 705–710.

Chan A, Carianopol C, Tsai AY, Varathanajah K, Chiu RS, Gazzarrini S. 2017. SnRK1 phosphorylation of FUSCA3 positively regulates embryogenesis, seed yield, and plant growth at high temperature in Arabidopsis. Journal of Experimental Botany **68,** 4219–4231.

Chen GX, Zhen SM, Liu YL, Yan X, Zhang M, Yan YM. 2017. In vivo phosphoproteome characterization reveals key starch granule-binding phosphoproteins involved in wheat water-deficit response. BMC Plant Biology **17,** 168.

Cherkasov V, Grousl T, Theer P, et al. 2015. Systemic control of protein synthesis through sequestration of translation and ribosome biogenesis factors during severe heat stress. FEBS Letters **589,** 3654–3664.

Chou MF, Schwartz D. 2011. Biological sequence motif discovery using *motif-x*. Current Protocols in Bioinformatics **35,** 13.15.1–13.15.24.

Cox J, Hein MY, Luber CA, Paron I, Nagaraj N, Mann M. 2014. Accurate proteome-wide label-free quantification by delayed normalization and maximal peptide ratio extraction, termed MaxLFQ. Molecular and Cellular Proteomics **13,** 2513–2526.

Cox J, Mann M. 2008. MaxQuant enables high peptide identification rates, individualized p.p.b.-range mass accuracies and proteome-wide protein quantification. Nature Biotechnology **26,** 1367–1372.

de Leonardis AM, Fragasso M, Beleggia R, Ficco DB, de Vita P, Mastrangelo AM. 2015. Effects of heat stress on metabolite accumulation and composition, and nutritional properties of durum wheat grain. International Journal of Molecular Sciences **16,** 30382–30404.

De Storme N, Geelen D. 2014. The impact of environmental stress on male reproductive development in plants: biological processes and molecular mechanisms. Plant, Cell and Environment **37,** 1–18.

de Zelicourt A, Colcombet J, Hirt H. 2016. The role of MAPK modules and ABA during abiotic stress signaling. Trends in Plant Science **21,** 677–685.

Ding Y, Li H, Zhang X, Xie Q, Gong Z, Yang S. 2015. OST1 kinase modulates freezing tolerance by enhancing ICE1 stability in Arabidopsis. Developmental Cell **32,** 278–289.

Dory M, Hatzimasoura E, Kállai BM, et al. 2018. Coevolving MAPK and PID phosphosites indicate an ancient environmental control of PIN auxin transporters in land plants. FEBS Letters **592,** 89–102.

Draeger T, Moore G. 2017. Short periods of high temperature during meiosis prevent normal meiotic progression and reduce grain number in hexaploid wheat (*Triticum aestivum* L.). Theoretical and Applied Genetics **130,** 1785–1800.

Dutta S, Mohanty S, Tripathy BC. 2009. Role of temperature stress on chloroplast biogenesis and protein import in pea. Plant Physiology **150,** 1050–1061.

Facette MR, Shen Z, Björnsdóttir FR, Briggs SP, Smith LG. 2013. Parallel proteomic and phosphoproteomic analyses of successive stages of maize leaf development. The Plant Cell **25,** 2798–2812.

Farooq M, Bramley H, Palta JA, Siddique KHM. 2011. Heat stress in wheat during reproductive and grain-filling phases. Critical Reviews in Plant Sciences **30,** 491–507.

Fischer RA. 1985. Number of kernels in wheat crops and the influence of solar radiation and temperature. Journal of Agricultural Science **105,** 447–461.

Franklin KA, Lee SH, Patel D, et al. 2011. Phytochrome-interacting factor 4 (PIF4) regulates auxin biosynthesis at high temperature. Proceedings of the National Academy of Sciences, USA **108,** 20231–20235.

Galli M, Liu Q, Moss BL, et al. 2015. Auxin signaling modules regulate maize inflorescence architecture. Proceedings of the National Academy of Sciences, USA **112,** 13372–13377.

Gallie DR, Le H, Caldwell C, Tanguay RL, Hoang NX, Browning KS. 1997. The phosphorylation state of translation initiation factors is regulated developmentally and following heat shock in wheat. Journal of Biological Chemistry **272,** 1046–1053.

Gan ES, Huang J, Ito T. 2013. Functional roles of histone modification, chromatin remodeling and microRNAs in Arabidopsis flower development. International Review of Cell and Molecular Biology **305,** 115–161.

Gray WM, Ostin A, Sandberg G, Romano CP, Estelle M. 1998. High temperature promotes auxin-mediated hypocotyl elongation in Arabidopsis. Proceedings of the National Academy of Sciences, USA **95,** 7197–202.

Gupta K, Sengupta A, Chakraborty M, Gupta B. 2016. Hydrogen peroxide and polyamines act as double edged swords in plant abiotic stress responses. Frontiers in Plant Science **7,** 1343.

Guy C, Kaplan F, Kopka J, Selbig J, Hincha DK. 2008. Metabolomics of temperature stress. Physiologia Plantarum **132,** 220–235.

Hasanuzzaman M, Nahar K, Alam MM, Roychowdhury R, Fujita M. 2013. Physiological, biochemical, and molecular mechanisms of heat stress tolerance in plants. International Journal of Molecular Sciences **14,** 9643–9684.

Hashiguchi A, Komatsu S. 2016. Impact of post-translational modifications of crop proteins under abiotic stress. Proteomes **4,** pii: E42.

Hawkesford MJ, Araus JL, Park R, Calderini D, Miralles D, Shen T, Zhang J, Parry MAJ. 2013. Prospects of doubling global wheat yields. Food and Energy Security **2,** 34–48.

Hayes S, Sharma A, Fraser DP, Trevisan M, Cragg-Barber CK, Tavridou E, Fankhauser C, Jenkins GI, Franklin KA. 2017. UV-B perceived by the UVR8 photoreceptor inhibits plant thermomorphogenesis. Current Biology **27,** 120–127.

Hedhly A, Hormaza JI, Herrero M. 2009. Global warming and sexual plant reproduction. Trends in Plant Science **14,** 30–36.

Hofmann NR, Theg SM. 2005. Chloroplast outer membrane protein targeting and insertion. Trends in Plant Science **10,** 450–457.

Huang F, Zago MK, Abas L, van Marion A, Galván-Ampudia CS, Offringa R. 2010. Phosphorylation of conserved PIN motifs directs Arabidopsis PIN1 polarity and auxin transport. The Plant Cell **22,** 1129–1142.

Ibañez C, Delker C, Martinez C, et al. 2018. Brassinosteroids dominate hormonal regulation of plant thermomorphogenesis via BZR1. Current Biology **28,** 303–310.e3.

International Wheat Genome Sequencing Consortium (IWGSC). 2014. A chromosome-based draft sequence of the hexaploid bread wheat (*Triticum aestivum*) genome. Science **345,** 1251788.

IPCC. 2014. Climate change 2014, Impacts, Adaptation, and Vulnerability. Organization & evironment. Contribution of Working Group III to the Fifth Assessment Report of the Intergovernmental Panel on Climate Change. Cambridge and New York: Cambridge University Press

Jagadish SV, Craufurd PQ, Wheeler TR. 2007. High temperature stress and spikelet fertility in rice (*Oryza sativa* L.). Journal of Experimental Botany **58,** 1627–1635.

Jia W, Li B, Li S, et al. 2016. Mitogen-activated protein kinase cascade MKK7–MPK6 plays important roles in plant development and regulates shoot branching by phosphorylating PIN1 in Arabidopsis. PLoS Biology **14,** e1002550.

Jung JH, Domijan M, Klose C, et al. 2016. Phytochromes function as thermosensors in Arabidopsis. Science **354,** 886–889.

Karijolich J, Yi C, Yu YT. 2015. Transcriptome-wide dynamics of RNA pseudouridylation. Nature Reviews. Molecular Cell Biology **16,** 581–585.

Ki D, Sasayama D, Cho HT. 2016. The M3 phosphorylation site is required for trafficking and biological roles of PIN-FORMED1, 2, and 7 in Arabidopsis. Frontiers in Plant Science **7,** 1479.

Kilisch M, Lytovchenko O, Arakel EC, Bertinetti D, Schwappach B. 2016. A dual phosphorylation switch controls 14-3-3-dependent cell surface expression of TASK-1. Journal of Cell Science **129,** 831–842.

Kim DH, Park MJ, Gwon GH, et al. 2014. An ankyrin repeat domain of AKR2 drives chloroplast targeting through coincident binding of two chloroplast lipids. Developmental Cell **30,** 598–609.

Kline KG, Barrett-Wilt GA, Sussman MR. 2010. In planta changes in protein phosphorylation induced by the plant hormone abscisic acid. Proceedings of the National Academy of Sciences **107,** 15986–15991.

Kosová K, Vítámvás P, Prášilová P, Prášil IT. 2013. Accumulation of WCS120 and DHN5 proteins in differently frost-tolerant wheat and barley cultivars grown under a broad temperature scale. Biologia Plantarum **57,** 105–112.

Kotak S, Larkindale J, Lee U, von Koskull-Döring P, Vierling E, Scharf KD. 2007. Complexity of the heat stress response in plants. Current Opinion in Plant Biology **10,** 310–316.

Kumar SV, Lucyshyn D, Jaeger KE, Alós E, Alvey E, Harberd NP, Wigge PA. 2012. Transcription factor PIF4 controls the thermosensory activation of flowering. Nature **484,** 242–245.

Kumar SV, Wigge PA. 2010. H2A.Z-containing nucleosomes mediate the thermosensory response in Arabidopsis. Cell **140,** 136–147.

Kumar V, Khare T, Sharma M, Wani S. 2017. Engineering crops for future: a phosphoproteomics approach. Current Protein and Peptide Science **18,** 1–1.

Laino P, Shelton D, Finnie C, De Leonardis AM, Mastrangelo AM, Svensson B, Lafiandra D, Masci S. 2010. Comparative proteome analysis of metabolic proteins from seeds of durum wheat (cv. Svevo) subjected to heat stress. Proteomics **10,** 2359–2368.

Lamberti G, Gügel IL, Meurer J, Soll J, Schwenkert S. 2011. The cytosolic kinases STY8, STY17, and STY46 are involved in chloroplast differentiation in Arabidopsis. Plant Physiology **157,** 70–85.

Lawrence M, Daujat S, Schneider R. 2016. Lateral thinking: how histone modifications regulate gene expression. Trends in Genetics **32,** 42–56.

Legris M, Klose C, Burgie ES, et al. 2016. Phytochrome B integrates light and temperature signals in Arabidopsis. Science **354,** 897–900.

Li H, Ding Y, Shi Y, Zhang X, Zhang S, Gong Z, Yang S. 2017. MPK3- and MPK6-mediated ICE1 phosphorylation negatively regulates ICE1 stability and freezing tolerance in Arabidopsis. Developmental Cell **43,** 630–642.e4.

Ling Q, Jarvis P. 2016. Analysis of protein import into chloroplasts isolated from stressed plants. Journal of Visualized Experiments **117,** doi: 10.3791/54717.

Liu Z, Xin M, Qin J, Peng H, Ni Z, Yao Y, Sun Q. 2015. Temporal transcriptome profiling reveals expression partitioning of homeologous genes contributing to heat and drought acclimation in wheat (*Triticum aestivum* L.). BMC Plant Biology **15,** 152.

Lu Y, Li R, Wang R, Wang X, Zheng W, Sun Q, Tong S, Dai S, Xu S. 2017. Comparative proteomic analysis of flag leaves reveals new insight into wheat heat adaptation. Frontiers in Plant Science **8,** 1086.

Luo MC, Gu YQ, Puiu D, et al. 2017. Genome sequence of the progenitor of the wheat D genome *Aegilops tauschii*. Nature **551,** 498–502.

Majoul T, Bancel E, Triboï E, Ben Hamida J, Branlard G. 2003. Proteomic analysis of the effect of heat stress on hexaploid wheat grain: characterization of heat-responsive proteins from total endosperm. Proteomics **3,** 175–183.

Merret R, Nagarajan VK, Carpentier MC, et al. 2015. Heat-induced ribosome pausing triggers mRNA co-translational decay in *Arabidopsis thaliana*. Nucleic Acids Research **43,** 4121–4132.

Mochida K, Shinozaki K. 2013. Unlocking Triticeae genomics to sustainably feed the future. Plant and Cell Physiology **54,** 1931–1950.

Nguyen TH, Brechenmacher L, Aldrich JT, et al. 2012. Quantitative phosphoproteomic analysis of soybean root hairs inoculated with *Bradyrhizobium japonicum*. Molecular and Cellular Proteomics **11,** 1140–1155.

Nishi H, Demir E, Panchenko AR. 2015. Crosstalk between signaling pathways provided by single and multiple protein phosphorylation sites. Journal of Molecular Biology **427,** 511–520.

Nussinov R, Tsai CJ, Xin F, Radivojac P. 2012. Allosteric post-translational modification codes. Trends in Biochemical Sciences **37,** 447–455.

O'Connor DL, Elton S, Ticchiarelli F, Hsia MM, Vogel JP, Leyser O. 2017. Cross-species functional diversity within the PIN auxin efflux protein family. eLife **6,** e31804.

Oikawa K, Yamasato A, Kong SG, Kasahara M, Nakai M, Takahashi F, Ogura Y, Kagawa T, Wada M. 2008. Chloroplast outer envelope protein CHUP1 is essential for chloroplast anchorage to the plasma membrane and chloroplast movement. Plant Physiology **148,** 829–842.

Pécrix Y, Rallo G, Folzer H, Cigna M, Gudin S, Le Bris M. 2011. Polyploidization mechanisms: temperature environment can induce diploid gamete formation in *Rosa* sp. Journal of Experimental Botany **62,** 3587–3597.

Pflum MK, Tong JK, Lane WS, Schreiber SL. 2001. Histone deacetylase 1 phosphorylation promotes enzymatic activity and complex formation. Journal of Biological Chemistry **276,** 47733–47741.

Porter JR, Gawith M. 1999. Temperatures and the growth and development of wheat: a review. European Journal of Agronomy **10,** 23–36.

Qi X, Xu W, Zhang J, Guo R, Zhao M, Hu L, Wang H, Dong H, Li Y. 2017. Physiological characteristics and metabolomics of transgenic wheat containing the maize C4 phosphoenolpyruvate carboxylase (PEPC) gene under high temperature stress. Protoplasma **254,** 1017–1030.

Quint M, Delker C, Franklin KA, Wigge PA, Halliday KJ, van Zanten M. 2016. Molecular and genetic control of plant thermomorphogenesis. Nature Plants **2,** 15190.

Rampitsch C, Bykova NV. 2012. The beginnings of crop phosphoproteomics: exploring early warning systems of stress. Frontiers in Plant Science **3,** 144.

Raschke A, Ibañez C, Ullrich KK, et al. 2015. Natural variants of ELF3 affect thermomorphogenesis by transcriptionally modulating PIF4-dependent auxin response genes. BMC Plant Biology **15,** 197.

Rizhsky L, Liang H, Shuman J, Shulaev V, Davletova S, Mittler R. 2004. When defense pathways collide. The response of Arabidopsis to a combination of drought and heat stress. Plant Physiology **134,** 1683–1696.

Ruan YL, Jin Y, Yang YJ, Li GJ, Boyer JS. 2010. Sugar input, metabolism, and signaling mediated by invertase: roles in development, yield potential, and response to drought and heat. Molecular Plant **3,** 942–955.

Rust MJ, Markson JS, Lane WS, Fisher DS, O'Shea EK. 2007. Ordered phosphorylation governs oscillation of a three-protein circadian clock. Science **318,** 809–812.

Saini HS, Sedgley M, Aspinall D. 1983. Effect of heat stress during floral development on pollen tube growth and ovary anatomy in wheat (*Triticum aestivum* L.). Australian Journal of Physiology **10,** 137–144.

Saini HS, Sedgley M, Aspinall D. 1984. Developmental anatomy in wheat of male sterility induced by heat stress, water deficit or abscisic acid. Australian Journal of Plant Physiology **11,** 243–253.

Salazar C, Höfer T. 2009. Multisite protein phosphorylation— from molecular mechanisms to kinetic models. FEBS Journal **276,** 3177–3198.

Scalabrin E, Radaelli M, Rizzato G, Bogani P, Buiatti M, Gambaro A, Capodaglio G. 2015. Metabolomic analysis of wild and transgenic *Nicotiana langsdorffii* plants exposed to abiotic stresses: unraveling metabolic responses. Analytical and Bioanalytical Chemistry **407,** 6357–6368.

Schmitz RJ, Tamada Y, Doyle MR, Zhang X, Amasino RM. 2009. Histone H2B deubiquitination is required for transcriptional activation of FLOWERING LOCUS C and for proper control of flowering in Arabidopsis. Plant Physiology **149,** 1196–1204.

Schönichen A, Webb BA, Jacobson MP, Barber DL. 2013. Considering protonation as a posttranslational modification regulating protein structure and function. Annual Review of Biophysics **42,** 289–314.

Shalgi R, Hurt JA, Krykbaeva I, Taipale M, Lindquist S, Burge CB. 2014. Widespread inhibition of posttranscriptional splicing shapes the cellular transcriptome following heat shock. Cell Reports **49,** 439–452.

Steffens A, Bräutigam A, Jakoby M, Hülskamp M. 2015. The BEACH domain protein SPIRRIG is essential for Arabidopsis salt stress tolerance and functions as a regulator of transcript stabilization and localization. PLoS Biology **13,** e1002188.

Strittmatter P, Soll J, Bölter B. 2010. The chloroplast protein import machinery: a review. Methods in Molecular Biology **619,** 307–321.

Sun J, Qi L, Li Y, Chu J, Li C. 2012. PIF4-mediated activation of YUCCA8 expression integrates temperature into the auxin pathway in regulating arabidopsis hypocotyl growth. PLoS Genetics **8,** e1002594.

Sun W, Van Montagu M, Verbruggen N. 2002. Small heat shock proteins and stress tolerance in plants. Biochimica et Biophysica Acta **1577,** 1–9.

Suzuki K, Takeda H, Tsukaguchi T, Egawa Y. 2001. Ultrastructural study on degeneration of tapetum in anther of snap bean (*Phaseolus vulgaris* L.) under heat stress. Sexual Plant Reproduction **13,** 293–299.

van Wijk KJ, Friso G, Walther D, Schulze WX. 2014. Meta-analysis of *Arabidopsis thaliana* phospho-proteomics data reveals compartmentalization of phosphorylation motifs. The Plant Cell **26,** 2367–2389.

Vignali M, Hassan AH, Neely KE, Workman JL. 2000. ATP-dependent chromatin-remodeling complexes. Molecular and Cellular Biology **20,** 1899–1910.

Vizcaíno JA, Csordas A, del-Toro N, et al. 2016. 2016 update of the PRIDE database and its related tools. Nucleic Acids Research **44,** D447–D456.

Vizcaíno JA, Deutsch EW, Wang R, et al. 2014. ProteomeXchange provides globally coordinated proteomics data submission and dissemination. Nature Biotechnology **32,** 223–226.

Vu LD, Stes E, Van Bel M, et al. 2016. Up-to-date workflow for plant (Phospho)proteomics identifies differential drought-responsive phosphorylation events in maize leaves. Journal of Proteome Research **15,** 4304–4317.

Vu LD, Verstraeten I, Stes E, Van Bel M, Coppens F, Gevaert K, De Smet I. 2017. Proteome profiling of wheat shoots from different cultivars. Frontiers in Plant Science **8,** 332.

Wagner D, Meyerowitz EM. 2002. SPLAYED, a novel SWI/SNF ATPase homolog, controls reproductive development in Arabidopsis. Current Biology **12,** 85–94.

Wang J, Li D, Shang F, Kang X. 2017. High temperature-induced production of unreduced pollen and its cytological effects in Populus. Scientific Reports **7,** 1–12.

Wang R, Zhang Y, Kieffer M, Yu H, Kepinski S, Estelle M. 2016*a*. HSP90 regulates temperature-dependent seedling growth in Arabidopsis by stabilizing the auxin co-receptor F-box protein TIR1. Nature Communications **7,** 10269.

Wang X, Xin C, Cai J, Zhou Q, Dai T, Cao W, Jiang D. 2016*b*. Heat priming induces trans-generational tolerance to high temperature stress in wheat. Frontiers in Plant Science **7,** 501.

Wardlaw IF, Dawson IA, Munibi P, Fewster R. 1989. The tolerance of wheat to high temperatures during reproductive growth. I. Survey procedures and general response patterns. Australian Journal of Agriculture Research **40,** 1–13.

Weller B, Zourelidou M, Frank L, Barbosa ICR, Fastner A, Richter S, Jürgens G, Hammes UZ, Schwechheimer C. 2017. Dynamic PIN-FORMED auxin efflux carrier phosphorylation at the plasma membrane controls auxin efflux-dependent growth. Proceedings of the National Academy of Sciences, USA **114,** E887–E896.

Wilkinson S. 1999. pH as a stress signal. Plant Growth Regulation **29,** 87–99.

Wu X, Gong F, Cao D, Hu X, Wang W. 2016. Advances in crop proteomics: PTMs of proteins under abiotic stress. Proteomics **16,** 847–865.

Xu D, Shan B, Lee BH, et al. 2015. Phosphorylation and activation of ubiquitin-specific protease-14 by Akt regulates the ubiquitin–proteasome system. eLife **4,** e10510.

Xu Y, Zhan C, Huang B. 2011. Heat shock proteins in association with heat tolerance in grasses. International Journal of Proteomics **2011,** 529648.

Xue GP, Sadat S, Drenth J, McIntyre CL. 2014. The heat shock factor family from *Triticum aestivum* in response to heat and other major abiotic stresses and their role in regulation of heat shock protein genes. Journal of Experimental Botany **65,** 539–557.

Yang F, Jørgensen AD, Li H, Søndergaard I, Finnie C, Svensson B, Jiang D, Wollenweber B, Jacobsen S. 2011. Implications of high-temperature events and water deficits on protein profiles in wheat (*Triticum aestivum* L. cv. Vinjett) grain. Proteomics **11,** 1684–1695.

Yang F, Melo-Braga MN, Larsen MR, Jørgensen HJ, Palmisano G. 2013. Battle through signaling between wheat and the fungal pathogen *Septoria tritici* revealed by proteomics and phosphoproteomics. Molecular and Cellular Proteomics **12,** 2497–2508.

Yu J, Han J, Kim Y-J, et al. 2017. Two rice receptor-like kinases maintain male fertility under changing temperatures. Proceedings of the National Academy of Sciences, USA **114,** 12327–12332.

Zhang M, Lv D, Ge P, Bian Y, Chen G, Zhu G, Li X, Yan Y. 2014*a*. Phosphoproteome analysis reveals new drought response and defense mechanisms of seedling leaves in bread wheat (*Triticum aestivum* L.). Journal of Proteomics **109,** 290–308.

Zhang M, Ma CY, Lv DW, Zhen SM, Li XH, Yan YM. 2014*b*. Comparative phosphoproteome analysis of the developing grains in bread wheat (*Triticum aestivum* L.) under well-watered and water-deficit conditions. Journal of Proteome Research **13,** 4281–4297.

Zhang N, Huo W, Zhang L, Chen F, Cui D. 2016. Identification of winter-responsive proteins in bread wheat using proteomics analysis and virus-induced gene silencing (VIGS). Molecular and Cellular Proteomics **15,** 2954–2969.

Zhang Y, Pan J, Huang X, et al. 2017. Differential effects of a post-anthesis heat stress on wheat (*Triticum aestivum* L.) grain proteome determined by iTRAQ. Scientific Reports **7,** 3468.

Zhao C, Wang P, Si T, et al. 2017. MAP kinase cascades regulate the cold response by modulating ICE1 protein stability. Developmental Cell **43,** 618–629.e5.

Zhao M, Yang S, Chen C-Y, Li C, Shan W, Lu W, Cui Y, Liu X, Wu K. 2015. Arabidopsis BREVIPEDICELLUS interacts with the SWI2/SNF2 chromatin remodeling ATPase BRAHMA to regulate KNAT2 and KNAT6 expression in control of inflorescence architecture. PLoS Genetics **11,** e1005125.

Zhen S, Deng X, Zhang M, Zhu G, Lv D, Wang Y, Zhu D, Yan Y. 2017. Comparative phosphoproteomic analysis under high-nitrogen fertilizer reveals central phosphoproteins promoting wheat grain starch and protein synthesis. Frontiers in Plant Science **8,** 67.

Zhu JK. 2016. Abiotic stress signaling and responses in plants. Cell **167,** 313–324.

Zinn KE, Tunc-Ozdemir M, Harper JF. 2010. Temperature stress and plant sexual reproduction: uncovering the weakest links. Journal of Experimental Botany **61,** 1959–1968.

Zourelidou M, Absmanner B, Weller B, et al. 2014. Auxin efflux by PIN-FORMED proteins is activated by two different protein kinases, D6 PROTEIN KINASE and PINOID. eLife **3,** e02860.